Polymer loaded microemulsions: Changeover from finite size effects to interfacial interactions

B. Kuttich, O. Ivanova, I. Grillo, and B. Stühn

Citation: J. Chem. Phys. **145**, 164904 (2016); doi: 10.1063/1.4966155
View online: http://dx.doi.org/10.1063/1.4966155
View Table of Contents: http://aip.scitation.org/toc/jcp/145/16
Published by the American Institute of Physics

Polymer loaded microemulsions: Changeover from finite size effects to interfacial interactions

B. Kuttich,[1,a)] O. Ivanova,[2] I. Grillo,[3] and B. Stühn[1]
[1]*Technische Universität Darmstadt, Darmstadt, Germany*
[2]*Jülich Centre for Neutron Science (JCNS) at Heinz Maier-Leibnitz Zentrum (MLZ), Forschungszentrum Jülich GmbH, Garching, Germany*
[3]*Institut Laue-Langevin (ILL), Grenoble, France*

(Received 28 July 2016; accepted 12 October 2016; published online 26 October 2016)

Form fluctuations of microemulsion droplets are observed in experiments using dielectric spectroscopy (DS) and neutron spin echo spectroscopy (NSE). Previous work on dioctyl sodium sulfosuccinate based water in oil microemulsions in the droplet phase has shown that adding a water soluble polymer (Polyethylene glycol $M = 1500$ g mol^{-1}) modifies these fluctuations. While for small droplet sizes (water core radius $r_c < 37$ Å) compared to the size of the polymer both methods consistently showed a reduction in the bending modulus of the surfactant shell as a result of polymer addition, dielectric spectroscopy suggests the opposite behaviour for large droplets. This observation is now confirmed by NSE experiments on large droplets. Structural changes due to polymer addition are qualitatively independent of droplet size. Dynamical properties, however, display a clear variation with the number of polymer chains per droplet, leading to the observed changes in the bending modulus. Furthermore, the contribution of structural and dynamical properties on the changes in bending modulus shifts in weight. With increasing droplet size, we initially find dominating finite size effects and a changeover to a system, where interactions between the confined polymer and the surfactant shell dominate the bending modulus. *Published by AIP Publishing.* [http://dx.doi.org/10.1063/1.4966155]

I. INTRODUCTION

Microemulsions in the droplet phase are a well suited system to provide a soft confining geometry in the nanometre range.[1–3] Due to this softness, the interactions between confinement and confined molecules operate in both directions. The structural and dynamical properties of the confinement will change by introducing guest molecules as well as the properties of the guest molecules will change when brought into confinement. Therefore, in order to define accurately the confining geometry, these changes have to be known precisely. A key parameter for the phase stability of the soft confining microemulsions is the bending modulus κ of the surfactant shell.[4,5] Neutron spin echo (NSE) spectroscopy determines the relaxation time and amplitude of form fluctuations of the surfactant layer. This is a direct access to the bending modulus. Dielectric spectroscopy on the other hand allows to study the dynamic percolation transition. The transition temperature is related to the extent of form fluctuations and therefore provides an independent second observation.[1,6–10]

In a recent publication, we applied both methods to determine the influence of the water soluble polymer polyethylene glycol on the bending modulus of a dioctyl sodium sulfosuccinate (AOT) surfactant layer in a water in oil microemulsion. The oil used was octane. The systems investigated by NSE had droplet radii of 17 Å and 26 Å. In the polymer free state, they were found to have a bending modulus around k_BT in accordance with literature.[1,9,11–13] The addition of polymer led to a significant reduction of the bending modulus, which was expressed in the dielectric spectroscopy results as a strong reduction of percolation temperatures. However, for larger droplets (with a radius above 37 Å) the percolation temperatures showed the opposite behaviour, increasing strongly under polymer addition. The reason for this change in response to the addition of polymer is unclear. In this present investigation, we will present NSE results for the modification of form fluctuations in large droplets with added polymer.

II. EXPERIMENTAL DETAILS

A. Sample preparation

Preparation of the different microemulsions was done by weighing the appropriate amounts of surfactant, water, oil, and polymer on a micro-balance and mixing of these components in a vortex shaker. The surfactant was obtained from Sigma Aldrich and dried for 24 h at 45 °C in a vacuum oven before sample preparation. For the neutron scattering experiments, deuterated water (Carl Roth), deuterated octane (euriso-top, 98%), and deuterated polymer (Polyethylene Glycol (PEG) 1500 g mol^{-1} from Polymer Source) were used without further purifications, while for the dielectric spectroscopy nondeuterated components were used. Parametrisation of the mixing ratios for the polymer free systems is achieved by

a)Electronic mail: B.Kuttich@fkp.physik.tu-darmstadt.de

the parameters W and ϕ, where W denotes the molar ratio of water to surfactant molecules and ϕ the volume fraction of water and surfactant to the whole volume. For droplet phase microemulsions, this parametrisation is very convenient since W is proportional to the droplet water core radius r_c and ϕ simply gives the droplet volume fraction.[14] To quantify the amount of polymer in the samples, the parameter Z is introduced, calculated by the average number of polymer chains per droplet. For our experiments, we kept ϕ constant at 0.1 and chose W to be 30 and 40 yielding water core radii of 42 Å and 56 Å approximately.[15] The influence of the polymer on the systems was investigated for $Z = 1$ and $Z = 3$, which leads to polymer water concentrations less than 1% and thus, way below the estimated overlap concentration of PEG_{1500} of 20%.[16] Due to the deuteration scheme, a pronounced scattering contrast is given by the surfactant tails (shell contrast) in neutron scattering experiments.

B. Small-angle neutron scattering (SANS)

Small-angle neutron scattering (SANS) experiments were performed at the instrument D33 of the Institut Laue-Langevin (ILL). Neutron wavelength was 6 Å ($\Delta\lambda/\lambda = 0.09$) and detector distances of 2 m and 5 m were used.[17] With this setup, scattering vectors $q = \frac{4\pi}{\lambda}\sin(\theta/2)$ (with scattering angle θ) from 0.007 $Å^{-1}$ to 0.5 $Å^{-1}$ were investigated. For a better solubility of the polymer, all neutron scattering experiments were performed at a temperature of 35 °C. Measured scattering data were radially averaged, background corrected by an empty beam and an empty cell measurement, and normalised to absolute intensities by measuring water.

The intensity scattered by the microemulsion droplets was analysed with a spherical core shell model. The form factor reads as follows:[18]

$$F(q) = r_c^3\Delta\rho_{cs}\frac{\sin(qr_c) - qr_c\cos(qr_c)}{(qr_c)^3} + R^3\Delta\rho_{sm}\frac{\sin(qR) - qR\cos(qR)}{(qR^3)}. \quad (1)$$

The core radius is given by r_c, while R denotes the complete droplet radius including the surfactant tails. The differences in scattering length densities (SLD) between core and surfactant $\Delta\rho_{cs}$ and surfactant and matrix $\Delta\rho_{sm}$ can be calculated from the literature values of the single components:[1] $SLD_w = 6.37 \cdot 10^{-6}$ $Å^{-2}$, $SLD_s = -1.0 \cdot 10^{-7}$ $Å^{-2}$, and $SLD_m = 6.42 \cdot 10^{-6}$ $Å^{-2}$. The relative polydispersity p of the core radius of the droplets is considered by a Schulz-Zimm distribution.[19] In addition, the instrumental resolution due to a wavelength spread is taken into account by a convolution of the calculated intensity with a Gaussian function of appropriate width.[20] A detailed description of data evaluation can be found elsewhere.[1]

C. Neutron spin echo spectroscopy

The neutron spin echo (NSE) spectroscopy experiments were performed on the J-NSE instrument at the Heinz Maier-Leibnitz Zentrum (MLZ) in Garching with an incident neutron wavelength of 8 Å covering a Fourier time range from 0.1 ns up to 35 ns for 6 momentum transfer values q from 0.03 $Å^{-1}$ to 0.13 $Å^{-1}$. Raw data were corrected for the background contribution by subtracting the signal of deuterated octane measured with equal statistics. The scattered intensity was determined over the whole detector area (^{3}He detector with 32×32 pixels on 1 cm^2) without subdividing of the signal into different zones.

The normalised intermediate scattering functions $J(q,t) = I(q,t)/I(q,0)$ measured by the NSE instrument were fitted globally for all investigated q values with a complex model taking droplet form fluctuations into account. If the microemulsion droplet is described by a spherical particle, its form fluctuations can be modelled by deviations from this spherical shape. These deviations can be expanded in spherical harmonics describing spherical fluctuation modes. The zero order mode, for example, is the so-called breathing mode which accounts for the droplets polydispersity. The contribution of higher order modes to the overall dynamics decreases rapidly and usually the expansion is restricted to second order fluctuations.[5,6] As in case of the small angle scattering, droplet polydispersity can be taken into account by a Schulz-Zimm distribution. The complete intermediate scattering function reads as[6]

$$I(q,t) = \left\langle \exp\left[-D_{tr}q^2t\right] V_s(\Delta\rho)^2\left[f_0(qR) + \sum_{l\geq 2}\frac{2l+1}{4\pi}f_l(qR)\langle|u_l|^2\rangle\exp\left(-\frac{t}{\tau_l}\right)\right]\right\rangle_R, \quad (2)$$

with

$$f_0(x) = j_0(x)^2 + j_0(x)\sum_{l\geq 2}\frac{2l+1}{4\pi}\langle|u_l|^2\rangle[2 - x^2 + l(l+1)]j_0(x) - 2xj_1(x),$$
$$f_l(x) = [(l+2)j_l(x) - xj_{l+1}(x)]^2.$$

The translational diffusion of droplets is quantified by D_{tr}, while amplitudes and relaxation times of the single modes are given by $\langle|u_l|^2\rangle$ and τ_l, respectively. For the radius of the fluctuating shell, the full droplet radius R as given in the core-shell form factor (Equation (1)) is used. If the expansion is restricted to second order fluctuations only, then D_{tr}, $\langle|u_2|^2\rangle$, and τ_2 are the only fitting parameters, since R and the polydispersity are known from small angle scattering. The

q dependence of the intermediate scattering function is fully described by the form factors $f_0(qR)$ and $f_1(qR)$ and thus all data sets obtained by one spin echo experiment can be fitted globally to the same three parameters which allow a very reliable determination.

III. RESULTS

A. SANS: Droplet structure

The scattering curves obtained by small angle neutron scattering are depicted in Figure 1. Due to the deuteration scheme, a pronounced shell contrast is observed. Profiles are grouped for each droplet size and colour denotes the average number of polymer chains per droplet. The most prominent difference between the curves is the change in the position of the minimum between the $W = 30$ and $W = 40$ samples. This is due to an increase in the droplet radius with a rising molar water to surfactant ratio W, resulting in a shift to smaller q values.[1,14] In contrast, the effect of polymer addition is only subtle and cannot be seen directly in the obtained scattering curves.

Fitting the core shell model (mentioned in Section II B) results in the full black curves also shown in Figure 1. Obviously the model provides a very good fit to our data. Since the droplet volume concentration is $\phi = 0.1$, the influence of the structure factor on the model is negligible and will not be discussed further. The interesting parameters are thus the radius of the core r_c, its polydispersity p, and the thickness of the surfactant shell d. The variation of these parameters with the number Z of polymer chains per droplet is depicted in Figure 2. In order to give a full overview of the structural properties of the system, we included our previous results on the systems with $W = 12$ and $W = 20$ as well.[1]

As observed before, the thickness of the AOT shell surrounding the droplets is independent from the droplet size and polymer content. The mean shell thickness averaged over all investigated samples is $d = 9.1\ \text{Å} \pm 0.1\ \text{Å}$. The droplet water core radius r_c shows a strong dependency on the mixing ratio W, as already mentioned above. For

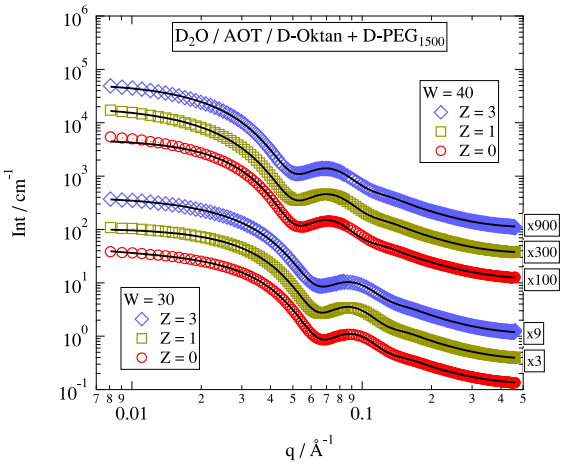

FIG. 1. SANS data and fitted model (full curves) for all investigated samples. Curves are shifted for clarity as indicated. Experimental errors are smaller than symbols.

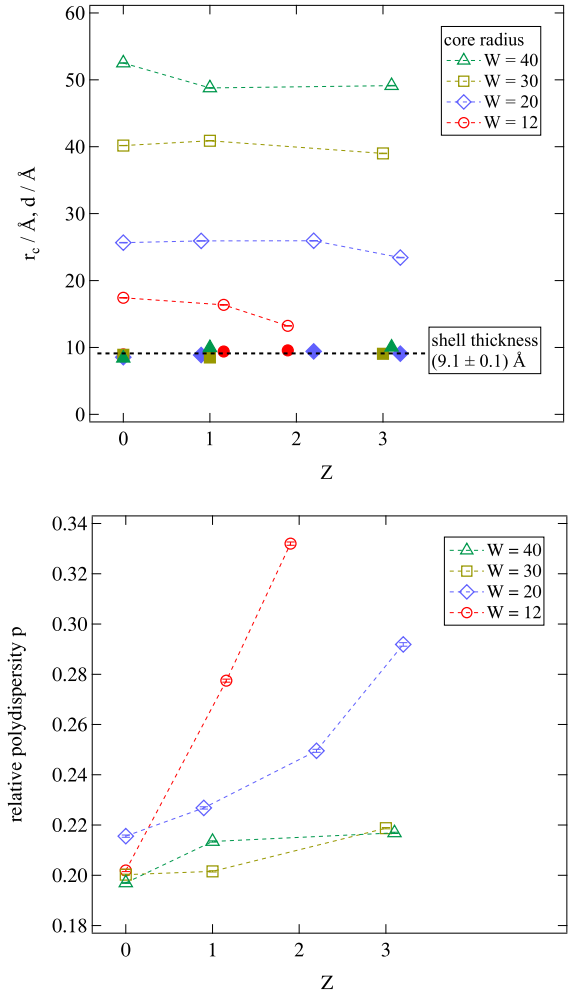

FIG. 2. Parameters deduced from the SANS fitting model for all samples with varying polymer content. Results from samples with $W = 12$ and $W = 20$ are taken from our previous publication.[1] Upper panel: droplet radii and shell thickness. Lower panel: polydispersity. Fitting errors are smaller than symbols.

the polymer free systems, r_c is proportional to W with a constant of proportionality of 1.3 Å, which is consistent with literature.[14,15,21] The droplet radius generally decreases with the addition of polymer while the relative changes are much stronger for small droplets. The radius of gyration of the used PEG_{1500} in water was determined to be $R_g = 10.8$ Å (data shown in the supplementary material). Thus the closer the droplet radius is to R_g, the stronger is the polymer influence on the droplet radius.[1]

The second parameter showing a strong influence on polymer addition is the polydispersity p of the core radius, shown in the lower panel of Fig. 2. For the small droplets investigated in our previous work, the polydispersity increases strongly, when polymer is added to the droplets. In cases of large droplets, this increase is almost insignificant, which corresponds well to the small polymeric influence on the droplet radius discussed before.

In conclusion, the addition of polymer to droplets with a core radius of $r_c \geq 40$ Å investigated in this work has only a very small impact on the structural properties of the microemulsions. Furthermore, the slight influence found for the droplet radius points towards the same direction

in comparison with the small droplets investigated in our previous work. Thus, from the structural point of view no reason for a changeover of the bending modulus, observed with dielectric spectroscopy, is seen.[1]

B. NSE: Form fluctuations

For the NSE experiments, the normalised intermediate scattering function $J(q,t)$ is analysed. Figure 3 depicts exemplarily the results for a polymer free and a polymer loaded system with $W = 30$. With increasing scattering vector q, the intermediate scattering function is decreasing faster. As emphasized by the dashed lines, a single exponential decay cannot describe the data properly.

The model used instead is based on the expansion of the droplet dynamics into spherical fluctuation modes as described in Section II C. If the expansion is restricted to zero and second order fluctuations only, the resulting $J(q,t)$ depends only on the droplet radius R, its polydispersity p as well as the relative amplitude u_2 and relaxation time τ_2 of the second mode. Due to the translational droplet diffusion, a fifth parameter D_{trans} has to be included. The droplet radius and its polydispersity are known from the SANS experiments discussed in Section III A; thus, only three free fitting parameters remain. These three parameters are independent of the scattering vector; thus, all data sets of a sample can be fitted globally with these three parameters only, reducing strongly fitting uncertainty.

In Figure 4, the results of the global fitting procedure for all investigated samples are shown. The translation diffusion coefficient is related to the hydrodynamic radius via the Stokes-Einstein relation and thus should be linked to the

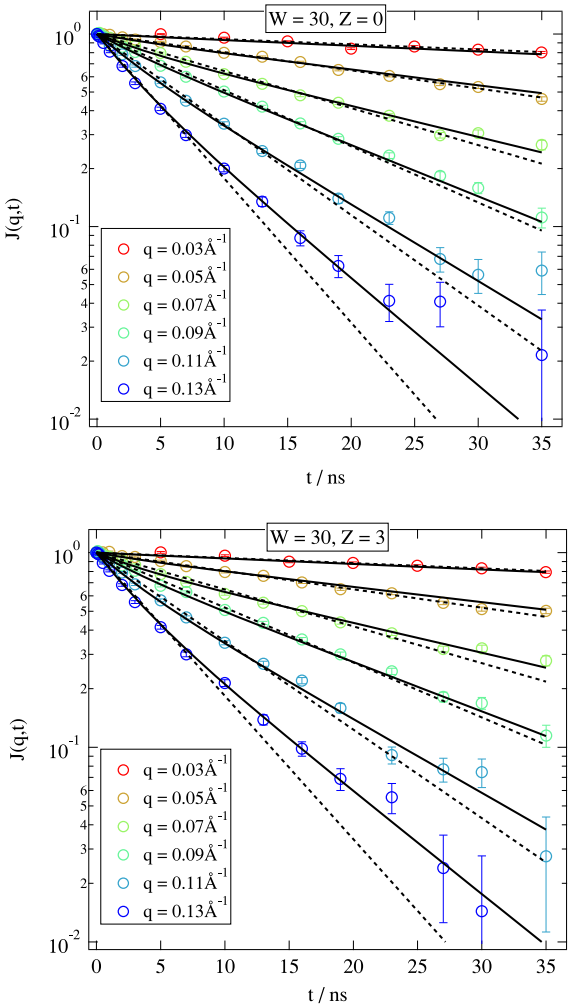

FIG. 3. Intermediate scattering functions for two different samples. Solid lines are fits with the model mentioned in Section II C. Dashed lines are fits with single exponential decays.

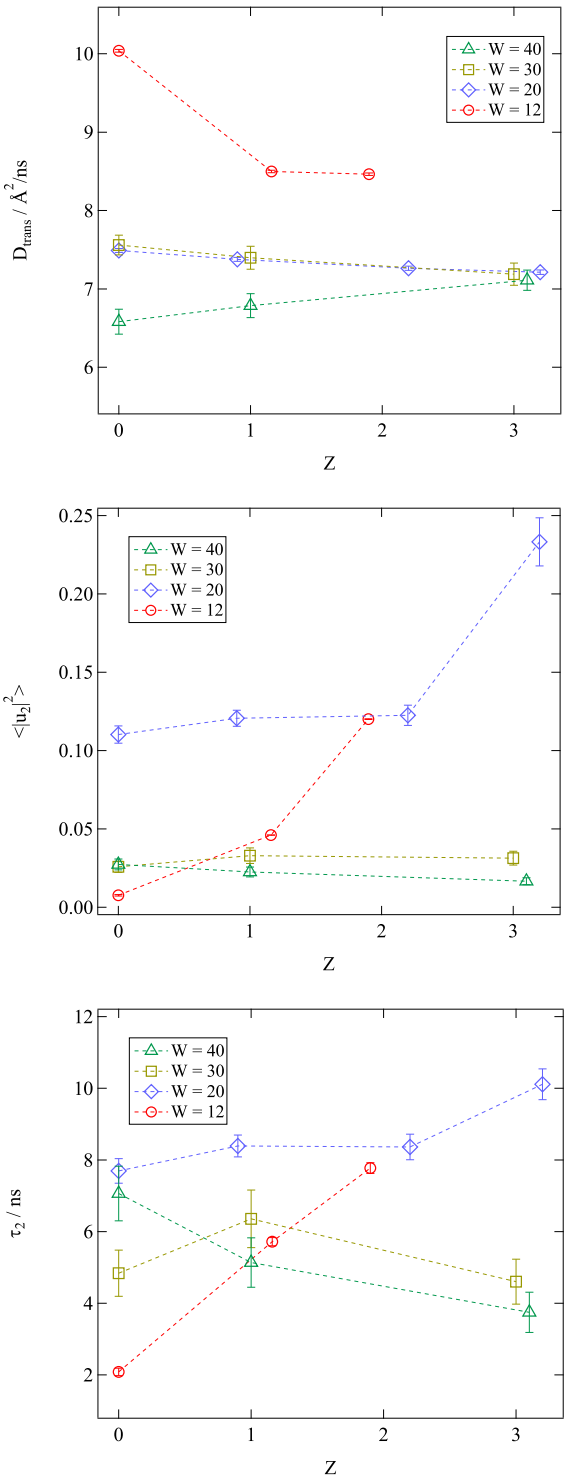

FIG. 4. Translational diffusion coefficient D_{trans}, dimensionless fluctuation amplitude of the second mode $\langle|u_2|^2\rangle$, and relaxation time of that mode τ_2 obtained from the fitting procedure.

droplet radius. Indeed, for the polymer free systems, a trend towards a higher diffusion coefficient for smaller droplets can be seen. Regarding the addition of polymer to the $W = 20$, $W = 30$, and $W = 40$ systems, the changes in the translational diffusion are weak. The absolute values of the $W = 20$ and $W = 30$ series are surprisingly close. For the smallest droplets, a tremendous reduction of the diffusion coefficient can be seen. This is surprising since the reduced droplet radius measured with SANS should lead to the opposite behaviour. Having a closer look into the SANS curves of the $W = 12$ system, discussed in our previous publication, reveals a strong increase in scattered intensity for small scattering vectors.[1] This indicates the emergence of droplet clusters, which we estimated to consist of approximately five droplets.[1] These clusters will have a strongly reduced translational diffusion coefficient which explains the observed trend for the $W = 12$ samples.

The second fitting parameter is the dimensionless amplitude of the second fluctuation mode. While the addition of polymer had a huge influence on this quantity for the small droplets investigated earlier, it has almost no impact for large droplets. The relaxation time τ_2 is of greater importance because it is directly linked to the bending modulus of the surfactant shell. The systems with intermediate droplet sizes ($W = 20$ and $W = 30$) show only minor changes in the relaxation time, while the $W = 12$ and $W = 40$ systems exhibit either a strongly increasing or decreasing relaxation time, respectively. Thus, while the structural changes of the $W = 40$ system discussed in Section III A are almost negligible, the relaxation time is affected strongly by polymer addition, in fact in the opposite direction as it is observed for the smallest droplets.

Finally, the results from SANS and NSE can be combined to calculate the bending modulus of the surfactant shell stabilising the droplets[7,8]

$$\kappa = \frac{1}{48}\left(\frac{k_B T}{\pi p^2} + \frac{\eta_w R^3}{\tau_2}\frac{23\eta_o + 32\eta_w}{3\eta_w}\right). \tag{3}$$

Droplet radius R and polydispersity p are known from SANS and relaxation time τ_2 from NSE. The temperature for the experiments was set to 308 K and the viscosities of water η_w and oil η_o were taken from literature.[22,23] Viscosity changes due to the presence of polymer in the water core are weak because of the low polymer concentration and are therefore not considered. In order to focus on the Z dependence of the bending modulus, Figure 5 depicts the normalised bending modulus, in which the normalisation was done by the bending modulus of the polymer free system according to the droplet radius.

The bending modulus decreases strongly for the smallest droplets investigated, while for the $W = 20$ series a decrease is only seen for the $Z = 3$ sample. For the large droplets, the behaviour is different. While the bending modulus for $W = 30$ samples stays almost constant, it increases significantly for $W = 40$. Investigating the reasons for this strong increase one can compare the influence of R, p, and τ_2 on the change in κ. Thus, for the $W = 40$ system, the structural parameters R and p point towards a reduction of the bending modulus from $Z = 0$ to $Z = 3$ by roughly 10%. The slowing down

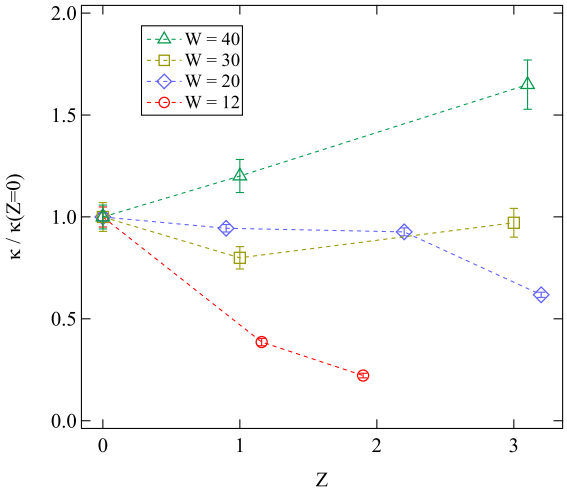

FIG. 5. Normalised bending modulus κ calculated from the combination of SANS and NSE results. To emphasise, the Z dependence data are normalised to the bending modulus of the polymer free system according to the droplet radius. Errors are smaller than symbols if not visible.

of the relaxation time τ_2 in contrast increases the bending modulus by 80%, leading in total to an increase in the bending modulus of 65%. Thus for the large droplet, the changes in the bending modulus are strongly dominated by the changes of the relaxation time. In case of the $W = 12$ samples, these contributions are different both leading to a reduction of κ. The changes in relaxation times are still the dominating parameters but with only 50% approximately, while R and p now account for roughly 25% each.

From the theory on droplet form fluctuations, it is possible to calculate polydispersity from the bending modulus and then in addition the amplitude of the second fluctuation mode.[5,24] These calculated values can then be compared to the measured one as sort of a consistency check of the used model. For all investigated systems except the $W = 12$ samples, both values agree well in a range of 20%. The deviations for the smallest droplets might be due to a nonvanishing saddle splay moment $\bar{\kappa}$, which is not considered in this work, and whose influence increases with increasing curvature of the surfactant shell.[4,24] A finite contribution of $\bar{\kappa}$ to the system's free energy will not change the polymeric influence on κ qualitatively. Due to the small sample set, a detailed investigation of $\bar{\kappa}$ is not done here.

The changeover from an increasing bending modulus due to the polymer addition for large droplets to a decreasing one for small droplets discussed above was already observed by dielectric spectroscopy.[1,25] To our knowledge in the framework of surfactant monolayers, this behaviour has not been investigated so far. However, for surfactant bilayers, composed, for example, of sodium dodecyl sulfate (SDS) a surfactant which is very similar to AOT, this phenomenon is also observed. While Brooks *et al.* deduced theoretically that a polymer adsorbed at a surfactant bilayer reduces the bending modulus, Iñiguez-Palomares *et al.* showed by dynamic light scattering that the addition of PEG strongly increases the bending modulus of a SDS bilayer.[26,27] The reason for the latter observation seems to be the fact that PEG not only adsorbs at the SDS head groups, but it is at least partially incorporated in the surfactant layer.[27–29] Due to the close similarity of

AOT and SDS, this incorporation is also likely for AOT monolayers. Furthermore, Shafir and Andelman analysed the free energy of a system composed of a polyelectrolyte and a charged surfactant membrane. For weak polymer surfactant interactions, they calculated a decreasing bending modulus if the salt concentration is high (c_{salt} = 0.1 M) and an increasing one if its lower.[30]

Although PEG is not a polyelectrolyte and a water/AOT/octane microemulsion does not form a surfactant bilayer, these results offer a possible explanation for our observations. We find that the presence of polymer has different effects on small and large droplets and that the changeover occurs at a droplet size which is not exclusively related to the size of the polymer.[1] For small droplets, the surfactant to water ratio and thus the concentration of dissociated sodium ions is higher than for the large ones, which might be a key parameter for the impact of the presence of PEG on the surfactant layer. On the other hand for small droplets, polymer size and droplet radii are close together leading to a confinement situation dominated by finite size effects.

IV. CONCLUSIONS

Extending our former work on the structure and dynamics of polymer loaded water in oil microemulsions to large droplet radii, we could now complement our investigations on this system.[1] The small angle neutron scattering showed that qualitatively structural changes due to the polymer addition are the same for all investigated droplet sizes. With increasing polymer content the core radius is almost constant, with a slightly decreasing tendency, while the thickness of the surfactant shell is unaffected. However, the relative polydispersity of the core radius is increased. Quantitatively the changes are more pronounced for small droplets, whose radius is close to the radius of gyration of the polymer.

Neutron spin echo spectroscopy resulted in intermediate scattering functions which displayed a clearly non-exponential decay. Taking droplet form fluctuations into account, expanding the dynamics in spherical relaxation modes results in a model which significantly improves the description of the measured data. For all NSE data, an expansion up to the second order mode was sufficient to fit our data. This was also found for the polymer loaded systems. For the determination of the bending modulus of the surfactant shell, the relaxation time τ_2 of this second mode is the relevant parameter. For the W = 30 series, it stayed almost constant while the larger droplets exhibited a strongly decreasing relaxation time upon polymer addition. For small droplets, the opposite behaviour was found.

Combining the structural and dynamical results, the bending modulus is calculated. The observed changes by the addition of polymer are dominated by an acceleration of the relaxation time for large droplets and a slowing down for the small ones. The observed behaviour fits nicely to our results with dielectric spectroscopy showing a decreasing or increasing percolation temperature, respectively. These different effects due to polymer addition are expected be caused by differences in the concentration of dissociated ions at the surfactant shell in small and large droplets. A second factor is the precise position of the polymer in the droplets as investigations on charged surfactant bilayers suggest.[30] To elucidate these assumptions further, a direct observation of the location of the polymer in the droplet and its conformation is needed.

SUPPLEMENTARY MATERIAL

See the supplementary material for intermediate scattering functions and fits of the remaining W = 30 and W = 40 samples not shown in the paper, as well as small angle neutron scattering on the used deuterated PEG_{1500} for the determination of the radius of gyration.

ACKNOWLEDGMENTS

Financial support by the "Deutsche Forschungsgemeinschaft" DFG through the "DFG-Forschergruppe 1583" by Project No. STU191/6-1 and the Jülich Centre of Neutron Research (JCNS) to perform the neutron scattering measurements at the Heinz Maier-Leibnitz Zentrum (MLZ), Garching, Germany is thankfully acknowledged.

[1]B. Kuttich, P. Falus, I. Grillo, and B. Stühn, J. Chem. Phys. **141**, 084903 (2014).
[2]M. Kotlarchyk, S. H. Chen, J. S. Huang, and M. W. Kim, Phys. Rev. A **29**, 2054 (1984).
[3]T. Spehr, B. Frick, I. Grillo, and B. Stühn, J. Phys.: Condens. Matter **20**, 104204 (2008).
[4]W. Helfrich, Z. Naturforsch. C **28**, 693 (1973).
[5]S. T. Milner and S. A. Safran, Phys. Rev. A **36**, 4371 (1987).
[6]B. Farago, D. Richter, J. S. Huang, S. A. Safran, and S. T. Milner, Phys. Rev. Lett. **65**, 3348 (1990).
[7]S. Komura and A. Seki, Physica A **192**, 27 (1993).
[8]Y. Kawabata, H. Seto, M. Nagao, and T. Takeda, J. Neutron Res. **10**, 131 (2002).
[9]W. Meier, Langmuir **12**, 1188 (1996).
[10]R. Wipf, S. Jaksch, and B. Stühn, Colloid Polym. Sci. **288**, 589 (2010).
[11]J. S. Huang, S. T. Milner, B. Farago, and D. Richter, Phys. Rev. Lett. **59**, 2600 (1987).
[12]B. P. Binks, J. Meunier, O. Abillon, and D. Langevin, Langmuir **5**, 415 (1989).
[13]E. van der Linden, S. Geiger, and D. Bedeaux, Phys. A **156**, 130 (1989).
[14]M. Kotlarchyk, S. H. Chen, and J. S. Huang, J. Phys. Chem. **86**, 3273 (1982).
[15]M. van Dijk, J. Joosten, Y. Levine, and D. Bedeaux, J. Phys. Chem. **93**, 2506 (1989).
[16]Q. Ying and B. Chu, Macromolecules **20**, 362 (1987).
[17]B. Kuttich, A. Matt, P. Falus, I. Hoffmann, I. Grillo, M. Gallei, and B. Stühn, "Polymer dynamics within microemulsion droplets," Institut Laue-Langevin (ILL), 2015.
[18]S. H. Chen, Annu. Rev. Phys. Chem. **37**, 351 (1986).
[19]M. Kotlarchyk, S. H. Chen, and J. S. Huang, Phys. Rev. A **28**, 508 (1983).
[20]J. S. Pedersen, D. Posselt, and K. Mortensen, J. Appl. Crystallogr. **23**, 321 (1990).
[21]M. Domschke, M. Kraska, R. Feile, and B. Stuhn, Soft Matter **9**, 11503 (2013).
[22]J. H. Dymond and H. A. Øye, J. Phys. Chem. Ref. Data **23**, 41 (1994).
[23]K. R. Harris and L. A. Woolf, J. Chem. Eng. Data **49**, 1064 (2004).
[24]B. Farago and M. Gradzielski, J. Chem. Phys. **114**, 10105 (2001).
[25]M. Appel, T. Spehr, R. Wipf, C. Moers, H. Frey, and B. Stühn, J. Chem. Phys. **139**, 184903 (2013).
[26]J. T. Brooks, C. M. Marques, and M. E. Cates, Europhys. Lett. **14**, 713 (1991).
[27]R. Iñiguez Palomares, H. Acuña Campa, and A. Maldonado, Phys. Rev. E **84**, 011604 (2011).
[28]M. I. Gjerde, W. Nerdal, and H. Høiland, J. Colloid Interface Sci. **183**, 285 (1996).
[29]B. Z. Shang, Z. Wang, and R. G. Larson, J. Phys. Chem. B **112**, 2888 (2008).
[30]A. Shafir and D. Andelman, Soft Matter **3**, 644 (2007).